Updated SAID analysis of pion photoproduction data

Ron L. Workman, William J. Briscoe, Mark W. Paris, and Igor I. Strakovsky

Institute for Nuclear Studies, Department of Physics, The George Washington University, Washington, DC 20052

Energy-dependent and single-energy fits to the existing pion photoproduction database have been updated to cover the region from threshold to 2.7 GeV in laboratory photon energy. Revised resonance photo-decay couplings have been extracted and compared to previous determinations. The influence of recent measurements is displayed. Remaining problems and future approaches are discussed.

I. INTRODUCTION

The SAID photoproduction analyses have been updated periodically since 1990 [1], with more frequent updates published through our web site [2]. Our last full analysis [3] has been revised twice [4,5] to include CLAS differential cross sections for neutral and charged pion production off proton targets. Some recent neutron target data were poorly predicted by these and the MAID [6] solutions, requiring changes in the neutron multipoles and resonance couplings. Further changes are expected with the incorporation of forthcoming data from JLab FROST [7] and HD-ICE [8], CB@MAMI [9], LEPS [10], and CB-ELSA [11]. Here we compare with previous fits and consider what changes can be expected with future additions to the database and changes in the SAID parametrization.

In Sec. II, we summarize changes to the SAID database. The changes reflected in our multipoles are displayed in Sec. III. A comparison of past and recent photo-decay amplitudes, for resonances giving a significant contribution to pion photoproduction, is made in Sec. IV. Finally, in Sec. V, we summarize our results and comment on possible changes owing to further measurements and changes in our parametrization form.

II. DATABASE

The most influential additions to our database have been recent measurements of the photon beam asymmetry Σ for $\vec{\gamma} n \rightarrow \pi^- p$ [12] and for $\vec{\gamma} n \rightarrow \pi^0 n$ [13] from GRAAL. These include 216 Σ measurements of $\pi^0 n$ covering $E_\gamma = 703$–1475 MeV and $\theta = 53°$–164° plus 99 Σ measurements of $\pi^- p$ for $E_\gamma = 753$–1439 MeV and $\theta = 33°$–163°.

We note that the GRAAL contribution to $\pi^0 n$ has doubled the world database for this reaction. Our best fit (SN11) for $\pi^0 n$ and $\pi^- p$, reduces the initial χ^2/data from 223 and 27 (for the SAID energy-dependent solution SP09 [4]) to 3.1 and 4.6, respectively. In particular, this shows that the $\pi^0 n$ data were not well predicted, based on the existing large proton-target database and the much smaller $\pi^- p$ dataset.

Cross-section [14,15], Σ [16,17], and double-polarized $C_{x'}$ [18] data for $\gamma p \rightarrow \pi^0 p$ have had a lesser impact. For this reason, in the next section we focus mainly on the neutron target fits and multipoles.

III. MULTIPOLE AMPLITUDES

The present multipole analysis retains the phenomenological form used in Ref. [3], which extended the multipole parametrization based on a Heitler K-matrix approach [1,19],

$$M = (\text{Born} + A)(1 + iT_{\pi N}) + BT_{\pi N}, \tag{1}$$

to include a term of the form

$$(C + iD)(\text{Im} T_{\pi N} - |T_{\pi N}|^2), \tag{2}$$

where $T_{\pi N}$ is the elastic πN scattering partial-wave amplitude associated with the pion-photoproduction multipole amplitude M. This new piece was found necessary to fit the increasingly precise polarization data and has recently been used in a study of the model-independence of energy-dependent and single-energy fits [20]. The factors A through D were parametrized in terms of simple polynomials with the correct threshold behavior. The Born and phenomenological (A) contributions are generally found to cancel, effectively reducing the Born contribution at higher energies. This was noted in Ref. [19]. The C and D term contribution grows with the πN reaction cross section and is shown, compared to the full amplitude, for representative multipoles in Fig. 1. The terms in Eqs. (1) and (2) satisfy Watson's theorem [21] below the two-pion production threshold, allowing for a smooth departure from this constraint at higher energies. Other forms, such as the Chew-Mandelstam (CM) parametrization [22],

$$M = \sum_\sigma [1 - \bar{K}C]_{\pi\sigma}^{-1} \bar{K}_{\sigma\gamma}, \tag{3}$$

employing CM K-matrix elements, $\bar{K}_{\pi\sigma}$, determined in a fit to πN elastic scattering data [23], have also been explored [22].

The multipole amplitudes are presented in terms of isospin states, as is the convention. Extending such an analysis below the $\pi^+ n$ threshold is clearly problematic. This region is not the focus of the present study and requires a separate analysis. In fits after SM95 [24], Arndt proposed a recipe whereby the above πN partial-wave T-matrices were evaluated in terms of the outgoing pion energy of a corresponding photoproduction reaction rather than the center-of-mass energy. This method allowed rather good fits to the threshold data, but resulted in a charge-state-dependent shift of the πN T-matrix pole positions, by a few MeV, depending on whether the $\pi^0 p$ or $\pi^+ n$ final states were being analyzed. Here we have made
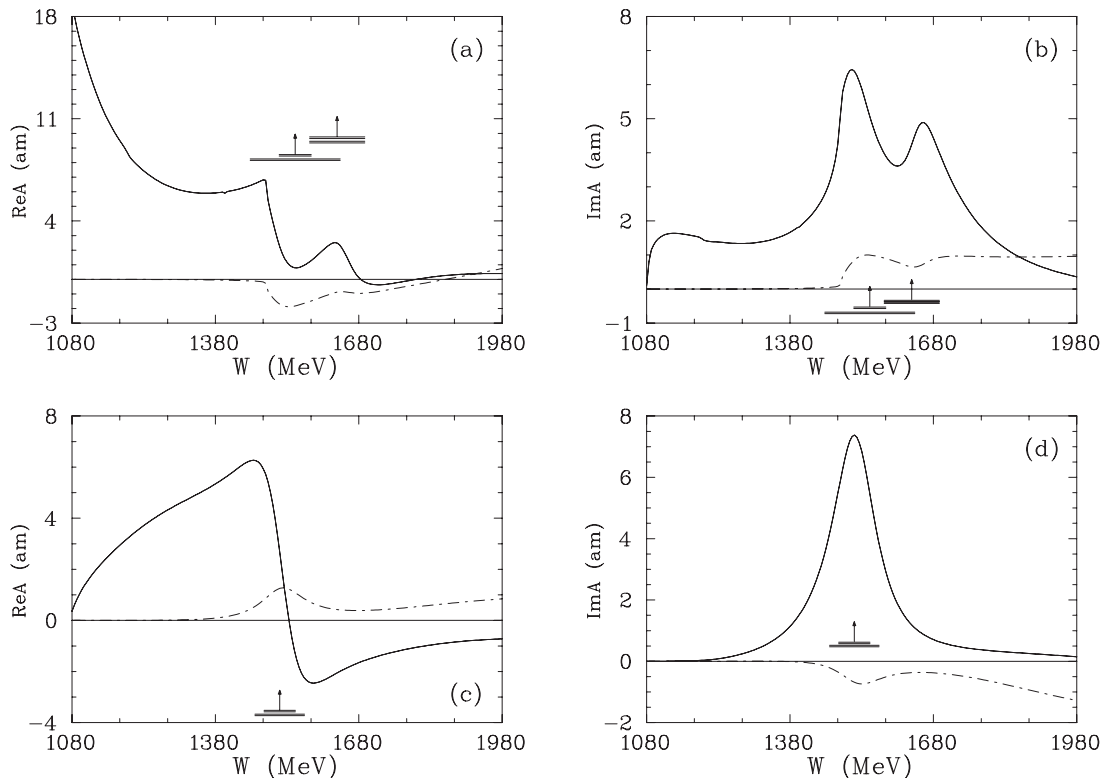
FIG. 1. Selected proton multipole amplitudes from threshold to $W = 2$ GeV ($E_\gamma = 1.68$ GeV). Solid (dash-dotted) lines correspond to the full SN11 solution (contribution of C and D terms). (a) Re($_p E_{0+}^{1/2}$), (b) Im($_p E_{0+}^{1/2}$), (c) Re($_p E_{2-}^{1/2}$), and (d) Im($_p E_{2-}^{1/2}$). Vertical arrows indicate resonance energies, W_R, and horizontal bars show full (Γ) and partial ($\Gamma_{\pi N}$) widths associated with the SAID πN solution SP06 [23].

fits, with (SK11) and without (SN11) this kinematic shift, to gauge its influence on the photodecay amplitudes. The fit quality, in terms of χ^2, for these and previous SAID solutions, is compared in Table I.

The SK11 fit extends down to the $\pi^0 p$ threshold, at a photon energy of $E_\gamma = 144.7$ MeV, while SN11 is limited to 155 MeV, just above the $\pi^+ n$ threshold (151.4 MeV), thus avoiding complications from the region between the $\pi^0 p$ and $\pi^+ n$ thresholds. The quality of the overall data fit, as shown in Table I, is nearly identical. As is described in Ref. [3], datasets are fitted to minimize the modified χ^2 function, given by

$$\chi^2 = \sum_j \left(\frac{X \theta_j - \theta_j^{\exp}}{\epsilon_j} \right)^2 + \left(\frac{X - 1}{\epsilon_X} \right)^2, \quad (4)$$

TABLE I. χ^2 comparison of fits to pion photoproduction data. Results are shown for eight different SAID solutions (current SN11 and SK11 with previous SP09 [4], FA06 [5], SM02 [3], and SM95 [24]). See text for details.

Solution	Energy limit (MeV)	χ^2/N_{Data}	N_{Data}
SN11	2700	2.08	25 553
SK11	2700	2.09	25 961
SP09	2700	2.11	25 639
SM02	2000	2.01	17 571
SM95	2000	2.37	13 415

where the subscript j labels data points within an angular distribution, $\theta_j^{\exp}$ is an individual measurement, θ_j is the calculated value, and ϵ_j is the statistical error. The factor X is used to scale angular distributions, with a systematic scaling uncertainty of ϵ_X. The full database χ^2 requires a sum over angular distributions, each having a separate value for ϵ_X. In Table II, we compare the fitted scale factors for the influential data of Refs. [12,13]. For some energies, the fit has chosen
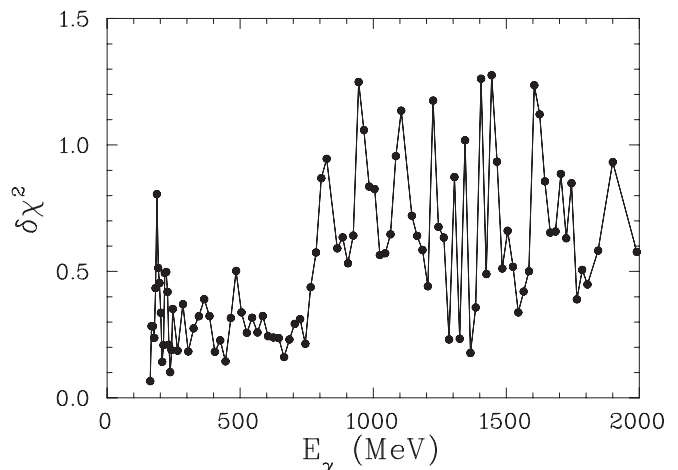
FIG. 2. (Color online) Comparison of the SES and global SN11 fits via $\delta\chi^2 = [\chi^2(\text{SN11}) - \chi^2(\text{SES})]/N_{\text{data}}$ versus laboratory photon energy E_γ.

TABLE II. Normalization factor for the recent GRAAL data vs SN11 solution. Systematic uncertainties for both sets are 4%. The upper set corresponds to the reaction $\vec{\gamma}n \rightarrow \pi^- p$ [12]. The lower set corresponds to the reaction $\vec{\gamma}n \rightarrow \pi^0 n$ [13].

Energy (MeV)	Norm
753.0	0.97
819.9	0.85
884.4	0.85
947.1	0.90
1006.5	0.92
1059.0	0.95
1100.4	0.89
1182.4	1.02
1259.4	1.03
1351.2	1.02
1438.9	0.90
702.6	0.95
734.1	1.01
769.9	0.97
799.4	0.91
826.9	0.90
861.8	0.93
895.5	0.95
929.3	1.01
962.4	1.05
991.2	1.06
1022.5	1.04
1053.8	1.07
1084.7	1.06
1112.8	1.01
1145.3	0.97
1174.8	0.97
1202.4	0.92
1231.7	0.92
1261.1	0.94
1288.3	0.94
1316.2	1.01
1343.7	0.94
1371.0	0.98
1398.1	0.99
1424.8	0.98
1449.0	1.03
1475.0	1.05

TABLE III. Resonance parameters for N^* and Δ^* states from the SAID fit to the πN data [23] (second column) and proton helicity amplitudes $A_{1/2}$ and $A_{3/2}$ (in $[(\text{GeV})^{-1/2} \times 10^{-3}]$ units) from the SN11 solution (first row), previous SP09 [4] solution (second row), and average values from the PDG10 [25] (third row).

Resonance	πN SAID	$A_{1/2}$	$A_{3/2}$
$N(1535)S_{11}$	$W_R = 1547$ MeV	99 ± 2	
	$\Gamma = 188$ MeV	100.9 ± 3.0	
	$\Gamma_\pi / \Gamma = 0.36$	90 ± 30	
$N(1650)S_{11}$	$W_R = 1635$ MeV	65 ± 25	
	$\Gamma = 115$ MeV	9.0 ± 9.1	
	$\Gamma_\pi / \Gamma = 1.00$	53 ± 16	
$N(1440)P_{11}$	$W_R = 1485$ MeV	-58 ± 1	
	$\Gamma = 284$ MeV	-56.4 ± 1.7	
	$\Gamma_\pi / \Gamma = 0.79$	-65 ± 4	
$N(1720)P_{13}$	$W_R = 1764$ MeV	99 ± 3	-43 ± 2
	$\Gamma = 210$ MeV	90.5 ± 3.3	-36.0 ± 3.9
	$\Gamma_\pi / \Gamma = 0.09$	18 ± 30	-19 ± 20
$N(1520)D_{13}$	$W_R = 1515$ MeV	-16 ± 2	156 ± 2
	$\Gamma = 104$ MeV	-26.0 ± 1.5	141.2 ± 1.7
	$\Gamma_\pi / \Gamma = 0.63$	-24 ± 9	166 ± 5
$N(1675)D_{15}$	$W_R = 1674$ MeV	13 ± 2	19 ± 2
	$\Gamma = 147$ MeV	14.9 ± 2.1	18.4 ± 2.1
	$\Gamma_\pi / \Gamma = 0.39$	19 ± 8	15 ± 9
$N(1680)F_{15}$	$W_R = 1680$ MeV	-13 ± 3	141 ± 3
	$\Gamma = 128$ MeV	-17.6 ± 1.5	134.2 ± 1.6
	$\Gamma_\pi / \Gamma = 0.70$	-15 ± 6	133 ± 12
$\Delta(1620)S_{31}$	$W_R = 1615$ MeV	64 ± 2	
	$\Gamma = 147$ MeV	47.2 ± 2.3	
	$\Gamma_\pi / \Gamma = 0.32$	27 ± 11	
$\Delta(1232)P_{33}$	$W_R = 1233$ MeV	-138 ± 3	-259 ± 5
	$\Gamma = 119$ MeV	-139.6 ± 1.8	-258.9 ± 2.3
	$\Gamma_\pi / \Gamma = 1.00$	-135 ± 6	-250 ± 8
$\Delta(1700)D_{33}$	$W_R = 1695$ MeV	109 ± 4	84 ± 2
	$\Gamma = 376$ MeV	118.3 ± 3.3	110.0 ± 3.5
	$\Gamma_\pi / \Gamma = 0.16$	104 ± 15	85 ± 22
$\Delta(1905)F_{35}$	$W_R = 1858$ MeV	9 ± 3	-46 ± 3
	$\Gamma = 321$ MeV	11.4 ± 8.0	-51.0 ± 8.0
	$\Gamma_\pi / \Gamma = 0.12$	26 ± 11	-45 ± 20
$\Delta(1950)F_{37}$	$W_R = 1921$ MeV	-71 ± 2	-92 ± 2
	$\Gamma = 271$ MeV	-71.5 ± 1.8	-94.7 ± 1.8
	$\Gamma_\pi / \Gamma = 0.47$	-76 ± 12	-97 ± 10

normalization factors significantly larger than 4%. We have repeated the fit without normalization freedom for the data sets listed in Table II. While this increases the χ^2 for these data by 20%, the multipole amplitudes do not change appreciably. Further fit details are available through the SAID web site [2] or from the authors.

We have generated the single-energy solutions (SES), described extensively in Refs. [3,20], based on the global fit SN11. The quantity $\delta\chi^2$ is the difference, $[\chi^2(\text{SN11}) - \chi^2(\text{SES})]$, divided by the number of data in each single-energy bin, providing a measure of the agreement between an individual SES and the global SN11 results (see Fig. 2).

Note that the values for $\delta\chi^2$ jump at about 800 MeV, which was the energy limit for MAMI-B, which produced a majority of the $\pi^0 p$ database. This is also close to the ηN production threshold. It is unclear whether this jump reflects an effect of the model or the overall data quality. We emphasize that the SES are generated mainly to search for missing structures in the global fit multipoles. Detailed comparisons of the global and SES fits can be made on the SAID web site [2].

In Fig. 3, we display the most significant deviations of the SN11 solution from the fit SP09, published in Ref. [4], and the Mainz MAID07 [6] result for selected neutron multipoles. The differences between our SN11 and SP09 results for neutron targets are visible particularly for the $E_{0+}^{1/2}$ (Fig. 3)
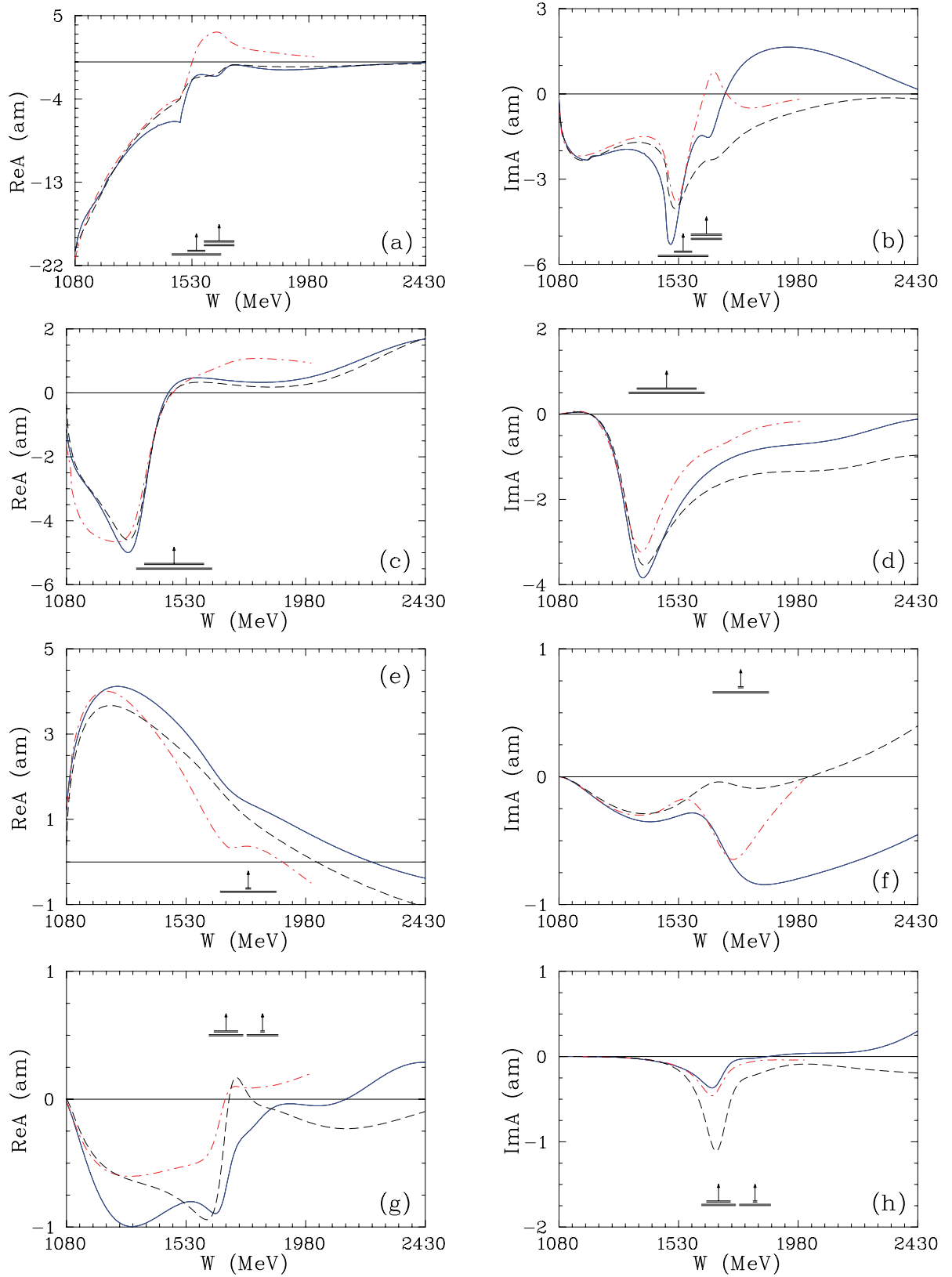
FIG. 3. (Color online) Selected neutron multipole amplitudes from threshold to $W = 2.43$ GeV ($E_\gamma = 2.7$ GeV). Solid lines correspond to the SN11 solution. Dashed (dash-dotted) lines give solution SP09 [4] (MAID07 [6], which terminates at $W = 2$ GeV). (a) Re($_nE_{0+}^{1/2}$), (b) Im($_nE_{0+}^{1/2}$), (c) Re($_nM_{1-}^{1/2}$), (d) Im($_nM_{1-}^{1/2}$), (e) Re($_nM_{1+}^{1/2}$), (f) Im($_nM_{1+}^{1/2}$), (g) Re($_nE_{3-}^{1/2}$), and (h) Im($_nE_{3-}^{1/2}$). Vertical arrows indicate W_R and horizontal bars show full (Γ) and partial ($\Gamma_{\pi N}$) widths associated with the SAID πN solution SP06 [23].
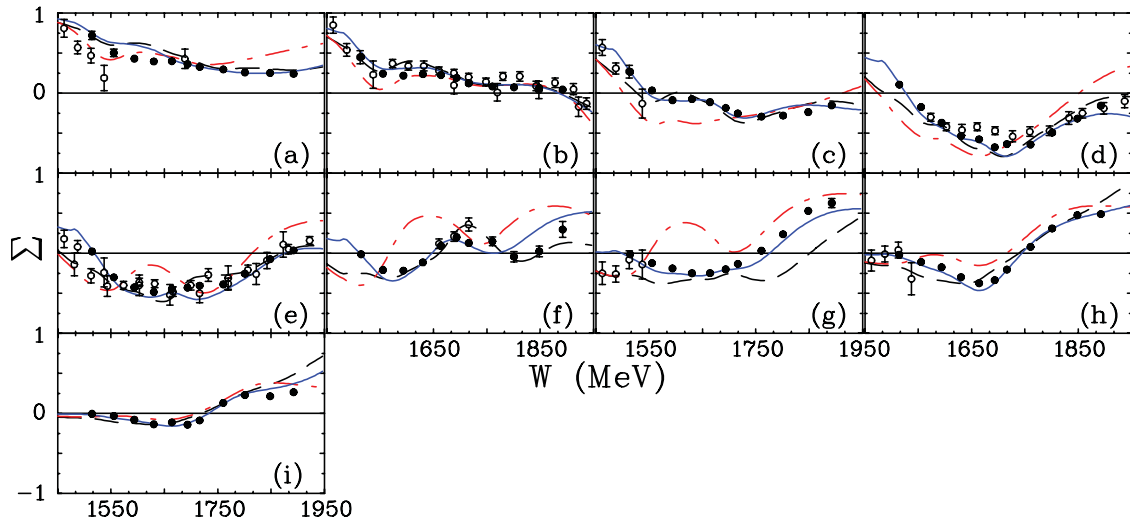
FIG. 4. (Color online) Σ-beam asymmetry for $\vec{\gamma}n \rightarrow \pi^- p$. Data (solid circles) are from GRAAL [12]. The previous measurements (open circles) are available in the SAID database [2]. (a) 34°, (b) 50°, (c) 67°, (d) 79°, (e) 90°, (f) 104°, (g) 128°, (h) 149°, and (i) 163°. Notation of the solutions is the same as in Fig. 3. GRAAL measurements are not included in SP09 and MAID07.

above $W \approx 1280$ MeV ($E_\gamma = 400$ MeV). The $E_{3-}^{1/2}$ multipole, connected to the $N(1680)F_{15}$ resonance, is also quite different. ($N(1680)$ being the Particle Data Group (PDG) notation [25] and $L_{2I,2J}$ being the associated notation for a state in πN elastic scattering [23].) The MAID07 fit was also modified [13] to accommodate the new $\pi^0 n$ Σ data, resulting in changes beginning at a higher energy, mainly altering the $N(1720)P_{13}$ resonance parameters. Fits to these neutron target data are displayed in Figs. 4 and 5.

In Figs. 6 and 7, we show discrepancies corresponding to the double-polarization quantity (G), at low energy, and others for the unpolarized cross section, at higher energies. In Fig. 7, we compare a prediction from SP09 to a fit including the data of Ref. [15]. A large discrepancy exists in the forward direction. Eliminating the existing CLAS cross sections [5], which do not extend to very forward angles, allows a slightly improved fit, but clearly does not resolve this problem, which exists also for the Bonn-Gatchina fits [28].

The Gerasimov-Drell-Hearn (GDH) integral is defined as

$$I_{\text{GDH}} = \int_{\nu_0}^{\infty} \frac{\sigma_{1/2} - \sigma_{3/2}}{\nu} d\nu = -\frac{\pi e^2}{2M^2}\kappa^2, \qquad (5)$$

where $\sigma_{1/2}$ and $\sigma_{3/2}$ are the photoabsorption cross sections for the helicity states 1/2 and 3/2, respectively, with ν being the photon energy. The result is expressible in terms of the charge, e, and the nucleon mass, M, and anomalous magnetic moment κ. Below, in Fig. 8, we display the effect this new solution has on the single-pion contribution to the GDH sum rule [29]. Extensive comparisons to data and other results were made in Ref. [3]. Here we compare the running integrals for several fits.

IV. RESONANCE COUPLINGS

To make meaningful comparisons [30] with previous resonance determinations, we have retained the method used in
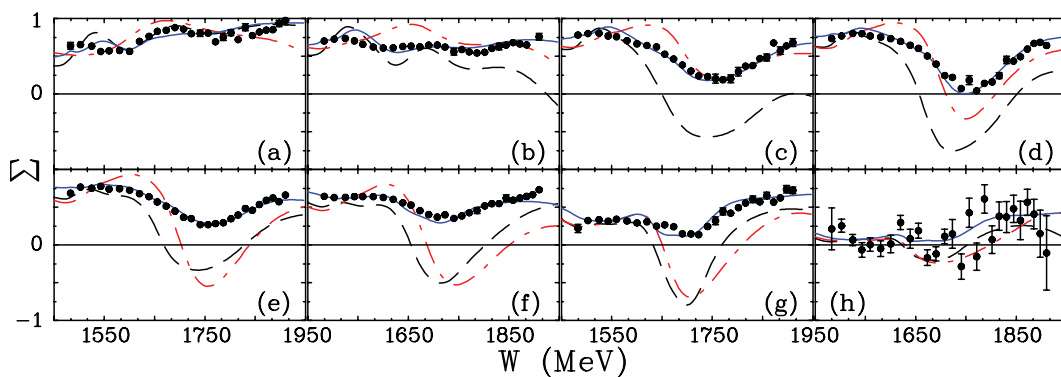
FIG. 5. (Color online) Σ-beam asymmetry for $\vec{\gamma}n \rightarrow \pi^0 n$. Data (filled circles) are from GRAAL [13]. (a) 54°, (b) 68°, (c) 80°, (d) 91°, (e) 105°, (f) 123°, (g) 144°, and (h) 163°. Notation of the solutions is the same as in Fig. 3. GRAAL measurements not included in SP09 and MAID07.
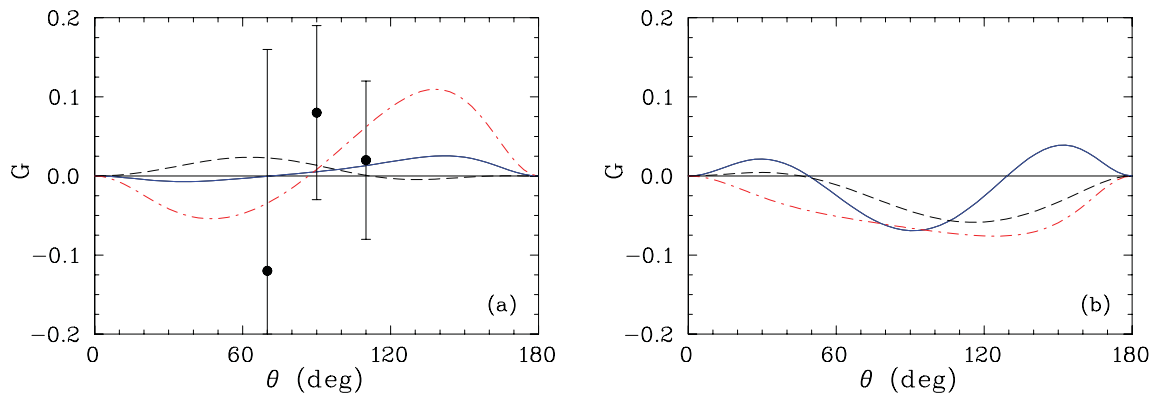
FIG. 6. (Color online) G asymmetry for neutral-pion photoproduction in the Δ resonance region ($E_\gamma = 340$ MeV). Data (solid circles) are from MAMI [26] (a) $\vec{\gamma}p \to \pi^0 p$ and (b) $\vec{\gamma}n \to \pi^0 n$. Notation of the solutions is the same as in Fig. 3.

Refs. [3–5], fitting the resultant multipoles with a background plus resonance assumption, similar to that used in the MAID analysis,

$$A(W)(1 + iT_{\pi N}) + T_{\mathrm{BW}} e^{i\phi}, \qquad (6)$$

wherein $T_{\pi N}$ is again the corresponding πN T matrix and T_{BW} is a Breit-Wigner (BW) parametrization of the resonance contribution. $A(W)$ is chosen to be a linear function of W.

Here the (theoretical) systematic error in our determination is generally much larger than the statistical errors found in fitting the data over an energy bin, around the BW resonance energy, or fitting (with subjective errors) the energy-dependent or single-energy multipoles covering the same energy range. The errors quoted in Tables III and IV were found by varying the energy range of the fit between the estimated resonance full and half-widths previously determined from our πN elastic scattering analysis [23].

The use of Eq. (6) in extracting the above values of $A_{1/2}$ and $A_{3/2}$ is reasonably consistent with the MAID approach, as

the Born terms are generally well-approximated by a linear function over narrow energy ranges covering a resonance. In our case, the function $A(W)$ is approximating the sum of background contributions from all terms in Eqs. (1) and (2). Good fits were found without need for a more complicated energy dependence.

In earlier extractions by Crawford and Morton [31], the background contribution was modeled by Born terms, multiplied by $(1 + iT_{\pi N})$, supplemented by a set of four polynomial and exponential functions having correct threshold behavior.

FIG. 7. (Color online) Differential cross section for $\gamma p \to \pi^0 p$ at $E_\gamma = 2225$ MeV. CLAS data (solid circles) are from [5]. CB-ELSA data (open circles [15] and solid triangles [27]). Notation of the solutions is the same as in Fig. 3. SZ11 solution (CLAS $\pi^0 p$ cross sections [4] excluded) is shown by a dotted line.

TABLE IV. Resonance parameters for N^* states from the SAID fit to the πN data [23] (second column) and neutron helicity amplitudes $A_{1/2}$ and $A_{3/2}$ (in $[(\mathrm{GeV})^{-1/2} \times 10^{-3}]$ units) from the SN11 solution (first row), previous SM02 [3] solution (second row), and average values from the PDG10 [25] (third row).

Resonance	πN SAID	$A_{1/2}$	$A_{3/2}$
$N(1535)S_{11}$	$W_R = 1547$ MeV	-60 ± 3	
	$\Gamma = 188$ MeV	-16 ± 5	
	$\Gamma_\pi / \Gamma = 0.36$	-46 ± 27	
$N(1650)S_{11}$	$W_R = 1635$ MeV	-26 ± 8	
	$\Gamma = 115$ MeV	-28 ± 4	
	$\Gamma_\pi / \Gamma = 1.00$	-15 ± 21	
$N(1440)P_{11}$	$W_R = 1485$ MeV	48 ± 4	
	$\Gamma = 284$ MeV	45 ± 15	
	$\Gamma_\pi / \Gamma = 0.79$	40 ± 10	
$N(1720)P_{13}$	$W_R = 1764$ MeV	-21 ± 4	-38 ± 7
	$\Gamma = 210$ MeV	$7 \pm 15^{\mathrm{a}}$	$-5 \pm 25^{\mathrm{a}}$
	$\Gamma_\pi / \Gamma = 0.09$	1 ± 15	-29 ± 61
$N(1520)D_{13}$	$W_R = 1515$ MeV	-47 ± 2	-125 ± 2
	$\Gamma = 104$ MeV	-67 ± 4	-112 ± 3
	$\Gamma_\pi / \Gamma = 0.63$	-59 ± 9	-139 ± 11
$N(1675)D_{15}$	$W_R = 1674$ MeV	-42 ± 2	-60 ± 2
	$\Gamma = 147$ MeV	-50 ± 4	-71 ± 5
	$\Gamma_\pi / \Gamma = 0.39$	-43 ± 12	-58 ± 13
$N(1680)F_{15}$	$W_R = 1680$ MeV	50 ± 4	-47 ± 2
	$\Gamma = 128$ MeV	29 ± 6	-58 ± 9
	$\Gamma_\pi / \Gamma = 0.70$	29 ± 10	-33 ± 9

$^{\mathrm{a}}$SM95 value [24].
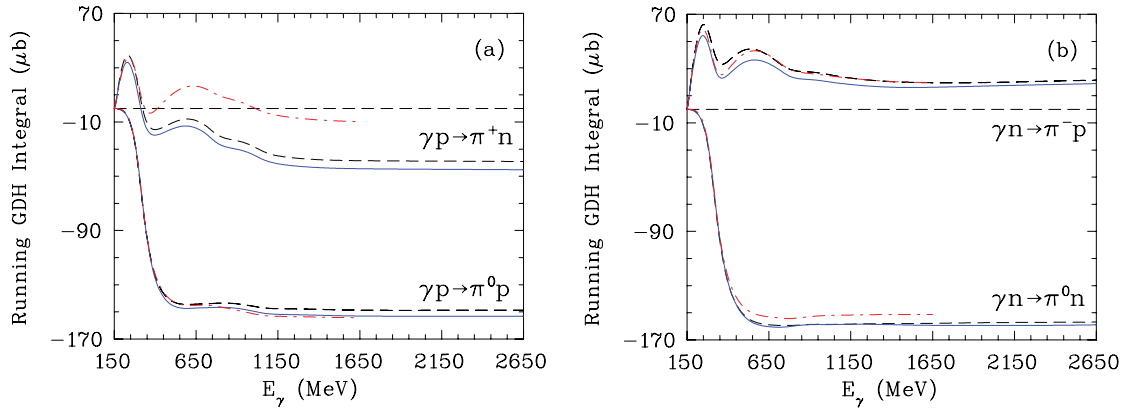
FIG. 8. (Color online) Running GDH integral for (a) proton and (b) neutron targets. Notation of the solutions is the same as in Fig. 3.

Born terms were not added if they made the fit more difficult. A similar approach was used in the fit of Berends and Donnachie [32], without the factor of $(1 + iT_{\pi N})$. Other more recent determinations [28] are based on the K- or T-matrix pole. The different approaches complicate comparisons, particularly for multipoles without clear resonance signatures.

The amplitudes $A_{1/2}$ and $A_{3/2}$ were determined assuming the masses, widths, and πN branching fractions determined in an earlier BW analysis of πN elastic scattering data [23]. In a few cases, these input parameters from πN scattering did not produce good fits to the photoproduction multipoles.

For the $N(1650)S_{11}$, increasing the mass to the nominal value of 1650 MeV produced a much better fit, as did increasing the width. The photo-decay couplings (proton and neutron) changed substantially and, as a result, this variability was taken to determine the quoted errors. The $N(1535)S_{11}$ decay to $p\gamma$ has remained quite stable while the decay to $n\gamma$ has changed significantly, due mainly to the new Σ data for both the $\pi^- p$ and $\pi^0 n$ channels, as shown in terms of the multipoles and data fits in Figs. 4 and 5.

The $N(1720)P_{13}$ neutron couplings are poorly determined, but the SN11 solution has, for the neutron $M_{1+}^{1/2}$ multipole, an imaginary part now more closely resembling the MAID07 value at the BW resonance energy. The MAID07 values for the neutron $A_{1/2}$ and $A_{3/2}$ amplitudes are -3 and -31 GeV$^{-1/2} \times 10^{-3}$, respectively, in better agreement with SAID, compared to the last published values from the SM95 fit. The $\Delta(1620)S_{31}$ amplitude is now significantly larger and outside of the PDG estimate, but is consistent with the MAID07 [6] and Bonn-Gatchina [28] results (66 and 63 ± 12 GeV$^{-1/2} \times 10^{-3}$, respectively).

V. SUMMARY AND CONCLUSION

This updated analysis examined mainly the effect of new neutron-target data on the SAID multipoles and resonance parameters. In some cases, the changes have been significant. The neutron multipoles generally show much larger variations than the proton multipoles, when the fits of different groups are compared. Given the inability of fits, based mainly on proton target data, to predict the $\pi^0 n$ multipoles, further changes can be expected as more neutron-target data become available.

Apart from a few special cases, the photodecay amplitudes, $A_{1/2}$ and $A_{3/2}$, found in this study are reasonably consistent with the PDG averages. Couplings for the states $\Delta(1600)P_{33}$ and $\Delta(1930)D_{35}$, which are weakly coupled to πN, have been reported in some older determinations [3,24], but are not found to be significant in the present study. The $N(1535)S_{11}$ and $N(1650)S_{11}$ amplitudes deserve further discussion, though they are now also consistent with the PDG estimates.

The large PDG uncertainty, assigned to the proton $N(1535)S_{11}$, was attributable mainly to a disagreement that existed between values determined from η photoproduction fits and existing values from pion photoproduction. Roughly, in 1995, the η photoproduction value for $A_{1/2}$ [33] was twice the SAID SM95 value from pion photoproduction. While the SAID value has migrated up to a value consistent with the early η photoproduction estimates, the MAID determination has decreased, once again leaving a wide discrepancy. The neutron coupling for the $N(1535)S_{11}$, which now is much larger in magnitude, is also consistent with a value determined in the Bonn-Gatchina [34] analysis of η photoproduction off the deuteron and closer to the MAID07 result. An increased SAID value for the proton $N(1650)S_{11}$ amplitude appears to be attributable more to the extraction technique than any change in the multipole. As we mentioned above, this extraction was very sensitive to assumed values for the mass and width, which may have produced the low value in Ref. [5].

Finally, we mention that preliminary fits to photoproduction data, using the CM formalism of Eq. (3), discussed in Ref. [22], are qualitatively similar to, but quantitatively different from, the results presented here. This form, which uses a more constrained approach to the incorporation of higher opening channels (ηN, $\pi \Delta$, ρN), essentially replaces the behavior of the term given in Eq. (2) (proportional to the reaction cross section) by terms contributing to each channel separately. A more detailed comparison is in progress.

[1] R. A. Arndt, R. L. Workman, Z. Li, and L. D. Roper, Phys. Rev. C **42**, 1853 (1990); **42**, 1864 (1990).

[2] The SAID web site contains data and fits for this and a number of other medium-energy reactions [http://gwdac.phys.gwu.edu].

[3] R. A. Arndt, W. J. Briscoe, I. I. Strakovsky, and R. L. Workman, Phys. Rev. C **66**, 055213 (2002).

[4] M. Dugger (CLAS Collaboration), Phys. Rev. C **79**, 065206 (2009).

[5] M. Dugger (CLAS Collaboration), Phys. Rev. C **76**, 025211 (2007).

[6] The MAID analyses are available through the Mainz web site [http://wwwkph.kph.uni-mainz.de/MAID/]. See also D. Drechsel, S. S. Kamalov, and L. Tiator, Eur. Phys. J. A **34**, 69 (2007).

[7] E. Pasyuk, Rapporter talk, *Baryon Spectroscopy with CLAS at Jefferson Lab*, 19th Particles and Nuclei International Conference (PANIC11), Cambridge, MA, USA, July 2011 [http://web.mit.edu/panic11/talks/monday/PARALLEL-1C/2-1400/pasyuk/404-0-Pasyuk_PANIC2011.pdf].

[8] F. Klein and A. Sandorfi (spokespersons), JLab Proposal E–06–101, Newport News, VA, 2006.

[9] H. J. Arends, Rapporter talk, *Highlights of N* Experiments at MAMI*, 8th International Workshop on the Physics of Excited Nucleons (NSTAR2011), Newport News, VA, USA, May, 2011 [http://www.jlab.org/conferences/Nstar2011/program.html].

[10] T. Nakano, Rapporter talk, *Highlights and Prospects from LEPS and LEPS2*, International Conference on the Structure of Baryons (BARYONS'10), Osaka, Japan, Dec. 2010 [http://www.rcnp.osaka-u.ac.jp/~baryons/program.html].

[11] F. Klein, Rapporter talk, *Highlights of N* Experiments at ELSA*, 8th International Workshop on the Physics of Excited Nucleons (NSTAR2011), Newport News, VA, May, 2011 [http://www.jlab.org/conferences/Nstar2011/program.html].

[12] G. Mandaglio (GRAAL Collaboration), Phys. Rev. C **82**, 045209 (2010); G. Giardina (private communication).

[13] R. Di Salvo (GRAAL Collaboration), Eur. Phys. J. A **42**, 151 (2009); G. Mandaglio (private communication).

[14] S. Schumann (Crystal Ball at MAMI, TAPS and A2 Collaborations), Eur. Phys. J. A **43**, 269 (2010).

[15] V. Crede (CBELSA/TAPS Collaboration), Phys. Rev. C **84**, 055203 (2011).

[16] D. Elsner (CB-ELSA and TAPS Collaborations), Eur. Phys. J. A **39**, 373 (2009).

[17] N. Sparks (CBELSA/TAPS Collaboration), Phys. Rev. C **81**, 065210 (2010).

[18] M. Sikora, Ph.D. thesis, Edinburgh University, 2011.

[19] R. L. Workman, Phys. Rev. C **74**, 055207 (2006).

[20] R. L. Workman, M. W. Paris, W. J. Briscoe, L. Tiator, S. Schumann, M. Ostrick, and S. S. Kamalov, Eur. Phys. J. A **47**, 143 (2011).

[21] K. M. Watson, Phys. Rev. **95**, 228 (1954).

[22] M. W. Paris and R. L. Workman, Phys. Rev. C **82**, 035202 (2010).

[23] R. A. Arndt, W. J. Briscoe, I. I. Strakovsky, and R. L. Workman, Phys. Rev. C **74**, 045205 (2006).

[24] R. A. Arndt, I. I. Strakovsky, and R. L. Workman, Phys. Rev. C **53**, 430 (1996).

[25] K. Nakamura (Particle Data Group), J. Phys. G **37**, 075021 (2010).

[26] J. Ahrens, S. Altieri, J. R. M. Annand, H. -J. Arends, R. Beck, A. Braghieri, N. d'Hose, H. Dutz, S. Goertz, P. Grabmayr *et al.*, Eur. Phys. J. A **26**, 135 (2005).

[27] O. Bartholomy (CB-ELSA Collaboration), Phys. Rev. Lett. **94**, 012003 (2005).

[28] A. V. Anisovich, E. Klempt, V. A. Nikonov, M. A. Matveev, A. V. Sarantsev, and U. Thoma, Eur. Phys. J. A **44**, 203 (2010); **47**, 27 (2011).

[29] S. B. Gerasimov, Phys. At. Nucl. (former Sov. J. Nucl. Phys.) **2**, 430 (1966); S. D. Drell and A. C. Hearn, Phys. Rev. Lett. **16**, 908 (1966); for an earlier related work, see L. I. Lapidus and Chou Kuang-chao, JETP (former Sov. J. Phys. JETP) **14**, 357 (1962).

[30] A more model-independent approach would have the comparison of pole residues. However, a comparison with the PDG and previous analyses would not be possible.

[31] R. L. Crawford and W. T. Morton, Nucl. Phys. B **211**, 1 (1983).

[32] F. A. Berends and A. Donnachie, Nucl. Phys. B **136**, 317 (1978).

[33] B. Krusche, J. Ahrens, G. Anton, R. Beck, M. Fuchs, A. R. Gabler, F. Härter, S. Hall, P. Harty, S. Hlavac, D. MacGregor, C. McGeorge, V. Metag, R. Owens, J. Peise, M. Röbig-Landau, A. Schubert, R. S. Simon, H. Ströher, and V. Tries, Phys. Rev. Lett. **74**, 3736 (1995).

[34] A. V. Anisovich, I. Jaegle, E. Klempt, B. Krusche, V. A. Nikonov, A. V. Sarantsev, and U. Thoma, Eur. Phys. J. A **41**, 13 (2009).